

Experimental Evaluation on Seismic Performance of Steel Trusses with Different Buckling-restrained Diagonal Members



T. Usami, J. Funayama & F. Imase

Department of Civil Engineering, Meijo University, Tempaku-ku, Nagoya 468-8502, Japan

C.-L. Wang

International Institute for Urban Systems Engineering, Southeast University, Sipailou 2#, Nanjing 210096, China

SUMMARY:

In order to verify the seismic performance of the steel truss bridge retrofitted by BRBs, an experiment was conducted by employing three steel truss specimens, whose configuration is regarded as part of steel truss bridge. These trusses had identical members except that they had the H-shaped diagonal braces, the H-shaped BRBs and the aluminum alloy BRB. Test results showed that the overall buckling of the H-shaped brace led to the failure of the truss and the damage to the bottom corner joints mainly resulted in the failure of the truss with BRBs. Moreover, the specimen with the H-shaped BRBs or the aluminum alloy BRBs exhibited the better ductility performance and dissipated more energy than the truss with the H-shaped diagonal braces. The failure displacement of the HBRB-C_y truss was about three times as large as the H-C_y truss.

Keywords: Steel Truss; Seismic Performance; Diagonal Braces; Buckling-restrained Brace; Aluminium Alloy

1. INTRODUCTION

Recent earthquakes have indicated the susceptibility of steel structures, including buildings and bridges, to various types of damage associated with large lateral deflections. To alleviate such problems, some research has been conducted to enhance the performance of steel structures under a strong earthquake excitation through the development of new structural configurations. Buckling-restrained braces (BRBs) were used to replace the structural braces because of their effective energy absorption mechanism and the relatively low cost (Watanabe et al., 1988; Uang et al., 2004). Previous numerical research showed that BRBs can improve the seismic performance of steel bridges as well as conventional building structures when they replace diagonal braces (Usami et al. 2005, Chen et al. 2011). Moreover, to guarantee the effective seismic performance of steel bridges, which might experience multiple earthquakes and aftershocks during their service life, steel and aluminum alloy high-performance BRBs (HPBRBs) had been developed (Usami et al. 2012, Wang et al. 2012).

Although the seismic performance of building structures retrofitted by the BRBs has been widely verified in the past few years (Tremblay et al., 2006; Tsai and Hsiao, 2008), few experiments about steel bridges have been given to verify the seismic behavior of steel bridges updated by BRBs. Recently, series of experimental studies on the scaled steel trusses with different conventional diagonal members or BRBs have been performed. These steel trusses are regarded as the part of steel truss bridges and designed by the specialized company. The purposes of these tests were to investigate the seismic performance and failure modes of steel trusses with the BRBs in contrast with steel trusses with the conventional diagonal braces. The difference among these tested trusses included: (1) V or inverted-V diagonal configuration; (2) the conventional diagonal members with tube or H sections; (3) the BRB with the plane core member manufactured by mild steel or aluminum alloy; (4) the BRB with the H-sectional core member; and (5) gusset plates with the different thickness. All of them had been done at Advanced Research Center for Seismic Experiments and Computations (ARCSEC) of Meijo University. In this paper, due to the limitation on space, test results of three truss specimens were given and they had the conventional H diagonal braces, the H-shaped BRB and the aluminum alloy

BRB, respectively.

2. TEST PROGRAM

2.1. Specimen's Configuration

As shown in Figure 1, this program investigated the behavior of two one-story, two-bay steel trusses, which were constructed as the substructure of steel truss bridges. The dimensions of three truss specimens were identical except for the diagonal braces. These specimens had a bay width of 800 mm and a height of 800 mm. The material of the $H100 \times 100 \times 6 \times 8$ member was the JIS grade SS400 steel except that the BRB's restrainers and gusset plates were made of the grade SM400 steel. Besides, the material of the aluminum alloy BRB was the JIS grade A6061S - T6. Table 1 lists the average values from the coupon tests. The test trusses were fabricated and assembled in the factory before testing.

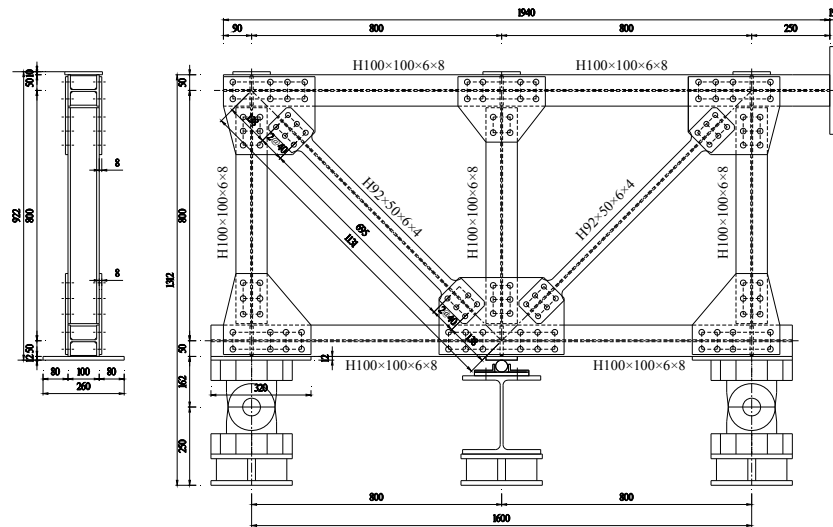


Figure 1. Overall view of test specimen

Table 1. Material Constants of Members

Member	Type	Thickness(mm)	E (GPa)	σ_y (MPa)	σ_u (MPa)	ϵ_u (%)	ν
Flange	SS400	7.6	210	314	452	28.4	0.285
Web	SS400	5.7	207	300	447	27.9	0.284
BRB's Restrainer	SM400	4.3	213	299	432	26.4	0.287
Plate (8mm)	SM400	8.0	209	289	425	27.5	0.288
Plate (4.5mm)	SM400	4.3	212	296	434	26.1	0.286
Aluminum alloy	A6061S-T6	10.0	72.1	273.8($\sigma_{0.2}$)	300.9	7.82	0.33

2.2. Descriptions of Diagonal Braces

The nominal dimensions of the H-shaped diagonal braces are given in Figure 2(a). The $H92 \times 50 \times 6 \times 4$ diagonal brace was manufactured from the $H100 \times 100 \times 6 \times 8$ formed steel by cutting its flanges' edges with a width of 25 mm and grinding its flanges with a thickness of 4 mm. Details of the geometric dimensions of the structural members are listed in Table 2.

A new type of BRB was employed in this experiment and the core brace member is H-shaped. So, this BRB was named H-shaped BRB or HBRB in this paper. In order to effectively restrain the local buckling of the flanges of the H-shaped diagonal brace, a U-shaped restrainer was developed. As

shown in Figure 2(b), two slim plates were welded to the U-shaped plate to constrain the local buckling of the flange together with plate restrainers, as shown in Figure 2(c). Two U-shaped restrainers and two plate restrainers were bolted together and formed a restraining system for the HBRB. As shown in Figure 2(a), some plate stiffeners were welded between the flanges' edges to prevent the buckling of the no-yielding portion of the brace member and the stoppers were welded at the center of the brace to prevent the slip-off movement of the restrainers. On the other hand, the same H-shaped braces were used as the conventional diagonal braces and the BRB's core member. It means that the H-shaped BRB can be manufactured from the original diagonal braces by restraining the buckling of the H-shaped braces. It was regarded as a new approach to decrease the retrofitting cost.

Furthermore, Figure 3 gives the dimensions of the aluminum alloy BRB. Two stiffeners are bolted on both ends of the BRB's brace member, and they were used to prevent the buckling of the no-yielding portion and avoid the welding, as discussed in the previous study (Usami et al, 2012).

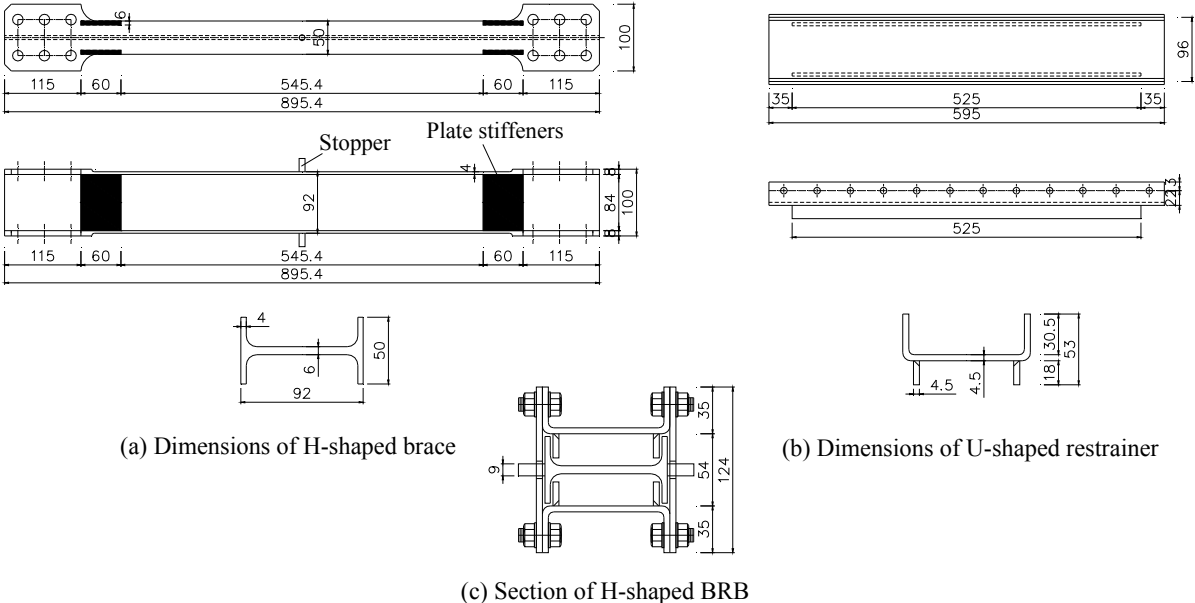


Figure 2. Details of H-shaped braces

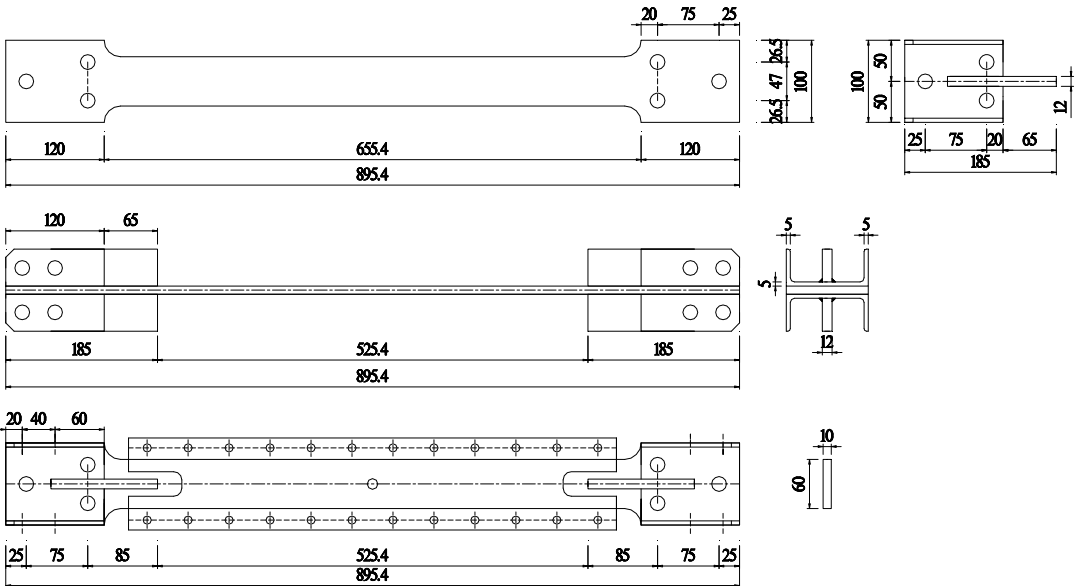


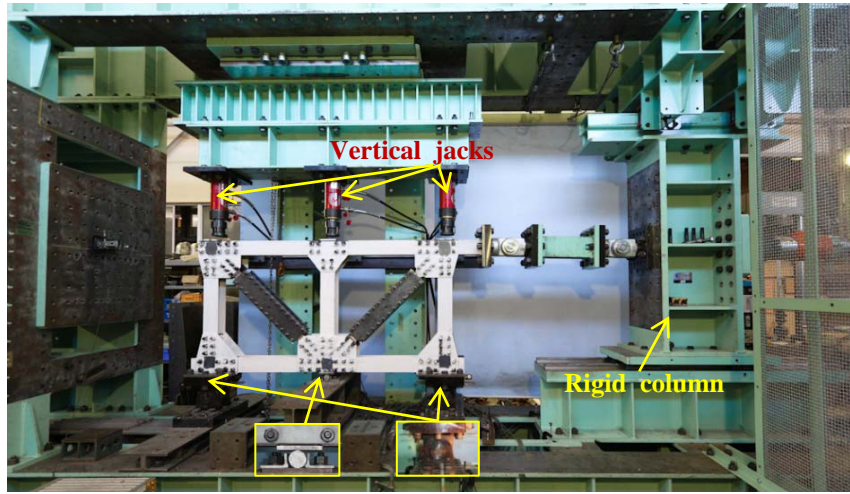
Figure 3. Details of aluminum alloy BRBs

Table 2. Geometric Dimensions of Structural Members

	H100×100×6×8	H92×50×6×4	PL60×10
Dimensions (mm)	$b=100; d=100; t_f=7.6; t_w=6.1$	$b=50.0; d=92; t_f=3.6; t_w=6.0$	$b=60.0; t=10.0$
Sectional Area (mm ²)	2037	869	600
i (mm)	25.0	9.38	2.89
N_y (kN)	630	266	164($N_{0.2}$)

2.3. Test Setup

As shown in Figure 4, a test truss specimen was vertically installed in a rigid test frame. The horizontal load was applied by one actuator. In order to simulate the design load of bridge decks, three constant loads were applied on the top of these vertical braces by three vertical actuators during all the loading histories. The left and right bottom corner joints of the steel truss were supported by hinges and they can only rotate in the truss's plane, which was obviously different with the previous experiments of the building structure installed with the BRBs. The middle bottom joint of the steel truss was located on a roller support. In order to prevent the out-of-plane movement of the test truss, lateral bracings were provided at three upper joints. One end of these bars was hinge-connected with the test specimen and the other end was supported by some blocks, which can move along the given fixed path. After the truss specimen was installed, it was whitewashed with a light coating of lime, which enhances the visibility of mill-scale flaking during the testing and indicates locations in the specimen where yielding occurred. So, some dark areas appeared in the following photos. The displacements of the truss or its members and the strain of the diagonal braces were monitored using transducers based on the need of the following discussion. Their values were collected by a digital data acquisition system.

**Figure 3.** Testing Setup

2.4. Loading Patterns

This experiment included one loading pattern. In the beginning of this loading pattern, three vertical actuators applied 132-kN compressive force to the truss specimen, respectively. The compressive forces were about twenty percent of the axial yield force of the vertical braces and were maintained throughout the following loading. Subsequently, the specified loading pattern was imposed by the horizontal actuator. It was the cyclic displacement history, which consisted of one cycle for each of the target displacements of 1, 2, 4, 6, 8, 10, 12, 14, 16, 20, 24, 28 and 36 mm. The two truss specimens with the HBRBs or the H-shaped braces tested under this loading history were named H-C_y and HBRB-C_y, respectively, where “C_y” indicates the cyclic displacement history. A similar loading pattern was employed on the test of the steel truss with the aluminum alloy BRB and this specimen was named ALBRB-C_y, where “ALBRB” indicates the aluminum alloy BRB.

3. TEST RESULTS

3.1. Observations of H-C_y Specimen

Figure 5 shows the horizontal force versus the drift relationship of the H-C_y specimen. At the positive and negative peaks of each cycle, the specimen was held in place for inspecting the yielding or fracture of the specimen. Furthermore, Figure 6 shows the main observations of the specimen during the loading.

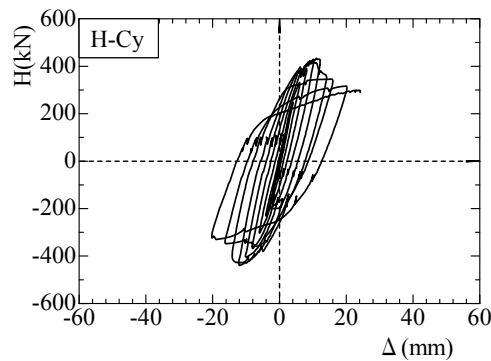


Figure 5. Hysteretic Curve of H-C_y Specimen

All the members of the specimen remained elastic during the first three loops ($\Delta=1$ mm, 2 mm and 4 mm). At the point of $\Delta= -6$ mm, the yielding of the flanges' edges was first seen on the left and right sides of the lower chord and on the bottom of the left vertical brace, as shown in Figure 6(a). In the following loops, the yielding of the flanges' edges occurred on the bottom of the middle and right vertical braces, and on the surfaces of the H-shaped diagonal braces. Especially, at $\Delta= -12$ mm, the hysteretic curve appeared stable and there is no clear deterioration in the relationship between the imposed displacement and the loading force. During the trip from $\Delta= -12$ mm to $\Delta= +14$ mm, a global buckling of the right diagonal brace corresponding to the first mode took place and the corresponding loading force suddenly dropped at $\Delta= +11.7$ mm, as shown in Figure 6(b). Moreover, during the trip from $\Delta= +14$ mm to $\Delta= -14$ mm, an overall buckling of the left diagonal brace corresponding to the second mode occurred and the corresponding force decreased. At $\Delta= +16$ mm, the local buckling of the flanges of the right diagonal brace were observed near the plate stiffeners; and some small cracks were observed at the weld toes between the flanges of the right lower chord and the base plate. At $\Delta= -16$ mm, the overall buckling of the left diagonal brace switched from the second mode to the first mode and some small local buckling of the flanges were observed on the left diagonal brace, as shown in Figure 6(c). Besides, the cracks were observed at the weld toes of the base plate. The deformation of the flanges around the left and right bottom corner joints was clear observed from the lime flaking. At $\Delta= +24$ mm, the crack near the welding of the plate stiffener on the right diagonal brace had grown large because of the low-cycle fatigue damage. So, the loading was stopped.

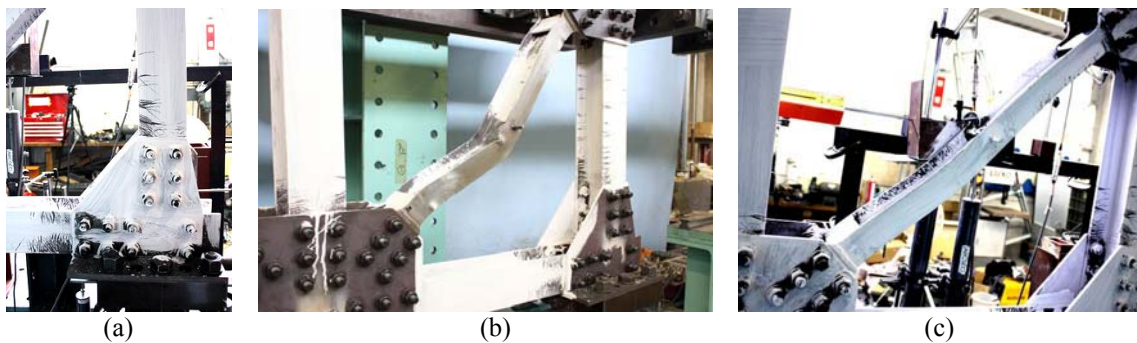


Figure 6. Deformation of H-C_y Specimen

3.2. Observations of HBRB-C_y Specimen

As shown in Figure 7, the HBRB-C_y specimen exhibited a stable hysteretic curve with the spindle shape. The load-carrying capacity of the specimen did not decrease until $\Delta = +28$ mm. Besides, the yielding and cracks of the flange, occurring in the lower chord and vertical braces, resulted in a loss in the strength.

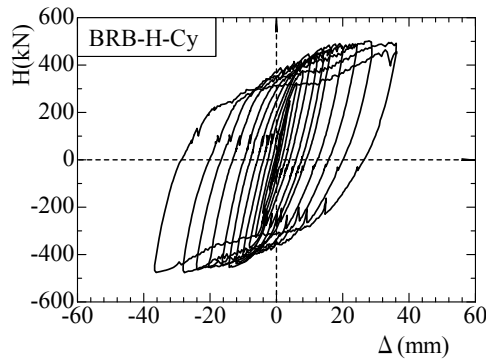


Figure 7. Hysteretic Curve of HBRB-C_y Specimen

At $\Delta = \pm 6$ mm, the yielding of the flanges occurred in the left and right lower chords and at the bottom of the left and right vertical braces. Moreover, At $\Delta = +8$ mm, the yielding of the flanges occurred in the middle vertical braces. At $\Delta = -14$ mm, cracks were observed on the weld toes of the left base plate, and at $\Delta = +20$ mm, cracks were observed on the weld toes of the right base plate. At $\Delta = \pm 36$ mm, cracks propagated from the bolt holes of the lower chord and left vertical brace nearest to the corner joints. It had grown large, as shown in Figure 7(a). At last, when the imposed displacement reached 36 mm again, the loading was stopped and the deformation of the specimen is presented in Figure 7(b).

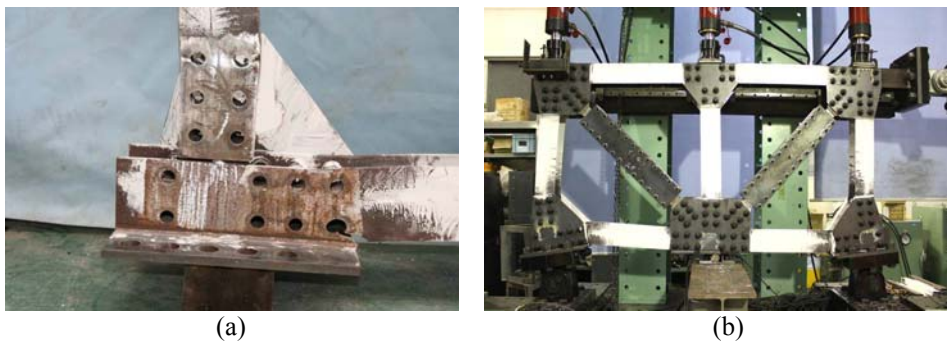


Figure 8. Damage of HBRB-C_y Specimen

3.3. Observations of ALBRB-C_y Specimen

As shown in Figure 9, the ALBRB-C_y specimen also exhibited a stable hysteretic curve with the spindle shape. The load-carrying capacity of the specimen did not decrease until $\Delta = +38$ mm. The yielding and cracks of the flange, occurring in the lower chord and vertical braces, resulted in a loss in the strength.

At $\Delta = \pm 8$ mm, the yielding of the flanges occurred in the left and right lower chords and at the bottom of the left vertical brace. Moreover, At $\Delta = -12$ mm, the yielding of the flanges occurred in the right vertical brace, and at $\Delta = +22$ mm, the yielding of the flanges occurred in the middle vertical brace. Moreover, at $\Delta = -22$ mm, cracks were observed on the weld toes of the left base plate, and at $\Delta = +38$ mm, cracks were observed on the weld toes of the right base plate. At $\Delta = \pm 48$ mm, cracks, located on

the weld toes of the base plates, propagated, as shown in Figure 10(a). Finally, when the local buckling of the BRB's brace member occurred, as shown in Figure 10(b), the loading was stopped.

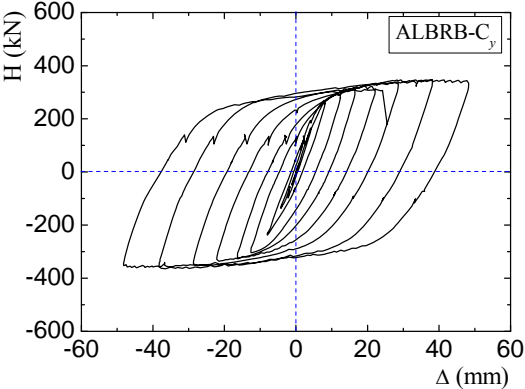


Figure 9. Hysteretic Curve of ALBRB-C_y Specimen

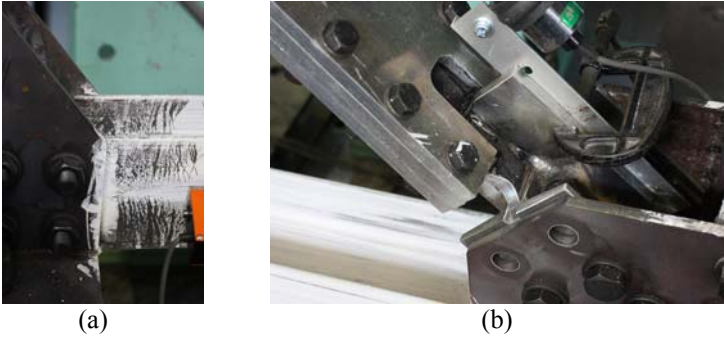


Figure 10. Damage of ALBRB-C_y Specimen

4. COMPARISON OF HYSTERETIC BEHAVIOR

In order to compare between the truss specimens, the average skeleton curves are given in Figure 11, which are the mean values of the bearing forces under the positive and negative amplitudes when the specimen was under the cyclic loading. Moreover, the failure points are defined when the ultimate bearing capacity of the specimen was decreased by 5%. So, the failure displacement Δ_{95} is also given corresponding to the failure points. In this experiment, the tests did not stop after the failure points and, actually, stopped according to the observation of the specimens' members.

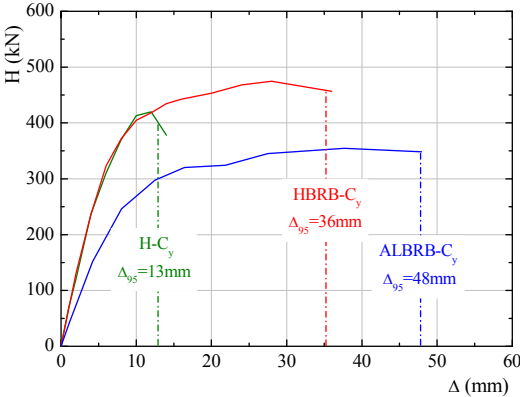


Figure 11. Skeleton Curves of Truss Specimens

As shown in Figure 11, the HBRB- C_y and ALBRB- C_y specimens exhibited the better ductility than the H- C_y specimen. The failure displacement of the HBRB- C_y specimen is about three times as large as the H- C_y specimen. Moreover, from the observation of these tests, the failure of the H- C_y specimen is due to the overall buckling of the diagonal brace, while the failure of the HBRB- C_y or ALBRB- C_y specimen is owing to the damage to the left and right bottom corner joints. The buckling of the diagonal brace quickly decreased the bearing capacity of the truss, which is obviously harmful to the bridge under the strong earthquake excitation. The damage to the corner joints was progressive so that the bearing capacity of the truss did not drop clearly. Besides, the HBRB- C_y and ALBRB- C_y specimens dissipated more energy than the H- C_y specimen.

5. CONCLUSIONS

In this paper, the experiment employing three steel trusses with the H-shaped diagonal braces, the H-shaped BRBs and the aluminium alloy BRBs has been conducted. Results are summarized here: (1) Test results shows that the steel truss with the BRBs exhibits the better performance and dissipates more energy than the steel truss with the H-shaped diagonal braces. (2) the overall buckling of the H-shaped brace led to the failure of the truss and the damage to the bottom corner joints mainly resulted in the failure of the truss with BRBs.

AKNOWLEDGEMENT

The study is supported by JSPS Grant-in-Aid for Scientific Research (B) 23360200 and in part by grants from Japan Science and Technology Agency for “Evaluation and Mitigation of Environment Impacts of Earthquake and Typhoon Disaster on Urban Area and Infrastructures” (Project Title: Refined Analysis and Damage Control of Earthquake Disaster Impact on Bridge Structures), under the Strategic Japanese-Chinese Cooperative Program on Science and Technology (S&T) for Environmental Conservation and Construction of a Society with Less Environmental Burden.

REFERENCES

- Chen X., Ge H.B. and Usami T. (2011). Seismic demand of buckling-restrained braces installed in steel arch bridges under repeated earthquakes. *Journal of Earthquake and Tsunami*, **5:2**, 119-150
- Tremblay, R., Bolduc, P., Neville, R. and DeVall, R. (2006). Seismic testing and performance of buckling-restrained bracing systems. *Canadian Journal of Civil Engineering*, **33:2**, 183-198.
- Tsai, K.-C. and Hsiao, P.-C. (2008). Pseudo-dynamic test of a full-scale CFT/BRB frame—part II: Seismic performance of buckling-restrained braces and connections. *Earthquake Engineering & Structural Dynamics*. **37:7**, 1099-1115.
- Uang, C.M., Nakashima, M. and Tsai K.C. (2004). Research and application of buckling-restrained braced frames. *International Journal of Steel Structure*. **4: 4**, 301-313.
- Usami, T., Lu Z.H. and Ge H.B. (2005). A seismic upgrading method for steel arch bridges using buckling-restrained braces. *Earthquake Engineering & Structural Dynamics*. **34: 4-5**, 471-496.
- Usami, T., Wang, C.-L. and Funayama, J. (2012). Developing high-performance aluminum alloy buckling-restrained braces based on series of low-cycle fatigue tests. *Earthquake Engineering & Structural Dynamics*. **41:4**, 643-661.
- Wang, C.-L., Usami, T. and Funayama, J. (2012). Evaluating the influence of stoppers on the low-cycle fatigue properties of high-performance buckling-restrained braces. *Engineering Structures*. **41**, 167-176.
- Watanabe, A., Hitomi, Y., Saeki, E., Wada, A. and Fujimoto, M. (1988). Properties of brace encased in buckling-restraining concrete and steel tube. *9th World Conference on Earthquake Engineering*: 719-724.